Journal of Molecular Catalysis A: Chemical 314 (2009) 81–87

Contents lists available at ScienceDirect

Journal of Molecular Catalysis A: Chemical

journal homepage: www.elsevier.com/locate/molcata

Methylation of naphthalene to prepare 2,6-dimethylnaphthalene over acid-dealuminated HZSM-12 zeolites

Xuefeng Bai[a,b], Keyi Sun[a], Wei Wu[a,*], Pengfei Yan[a], Jie Yang[a]

[a] Key Laboratory of Functional Inorganic Material Chemistry, Heilongjiang University, Ministry of Education, Sino-Russan Joint Laboratory for Catalysis, Harbin 150080, Heilongjiang, China
[b] Heilongjiang Institute of Petrochemistry, Harbin 150040, Heilongjiang, China

ARTICLE INFO

Article history:
Received 7 December 2008
Received in revised form 19 August 2009
Accepted 21 August 2009
Available online 29 August 2009

Keywords:
HZSM-12 zeolite
Acid dealumination
Methylation
2,6-Dimethylnaphthalene

ABSTRACT

The dealumination of HZSM-12 zeolite (Si/Al = 65) was carried out with citric acid and hydrochloric acid. The structure and acidity were characterized by XRD, XRF, SEM, N_2-adsorption, NH_3-TPD, Py-IR and ^{29}Si MAS NMR. The zeolites' catalytic properties were studied using the methylation of naphthalene to prepare 2,6-dimethylnaphthalene as a test reaction. The results show that the two kinds of acid can remove the framework Al of and decrease the amount of Brønsted acid sites, while not destroying the framework structure of the zeolite under the proper conditions. Hydrochloric acid removed both the strong and weak acid sites simultaneously, resulting in improved catalytic stability in the methylation of naphthalene (NAPH). In contrast, the citric acid preferred to remove the strongly acid sites and also formed secondary mesopores in the sample, resulting in improved reaction performance. Under the proper reaction conditions including: a reaction temperature of 350 °C, a reaction pressure of 4 MPa, a nitrogen flow rate of 10 mL/min, NAPH:CH_3OH:1,2,4-TMB 1:2:8 (mol), and WSHV = 3 h^{-1} with a reaction time of 4 h, the conversion of naphthalene was 30.5% and the ratio of 2,6-/2,7-DMN was 1.83 over dealuminated HZSM-12 by 10 mol/L hydrochloric acid for 6 h.

1. Introduction

2,6-Dimethylnaphthalene (2,6-DMN) is an important precursor of 2,6-naphthalene dicarboxylic acid, which is used as a monomer of polyethylene naphthalates (PEN) [1]. Compared with polytrimethylene terephthalate (PET), PEN has excellent properties as a gas barrier, as well as thermal and chemical stability, and mechanical properties leading to its wide application in electronics components, insulation material, food containers, aviation, and atomic energy materials. The multistep B.P-Amoco process, which involves four successive reactions starting from o-xylene and butadiene, has already been commercialized. However, it has the disadvantages of being environmentally unfriendly, a difficult process to execute and expensive, which greatly limits its application in industry. The process to prepare 2,6-DMN by alkylation of naphthalene with methanol is the most reasonable route for new technology. However, finding a high-yielding single-pot, selective method for preparing 2,6-DMN still remains an elusive goal because the products of methylation of naphthalene are very complicated, e.g., dimethylnaphthalene has 10 different isomers, and the difference in the boiling points of the isomers is extremely small: there is only a difference of 0.3 °C between the boiling points of 2,6-DMN and 2,7-DMN. Therefore, developing a highly selective catalyst is the key to realizing improved efficiency in the 2,6-DMN industry.

Zeolites are environmental friendly catalysts with designable porous structures and surface acidity that allows for improved selectivity for the desired products. The ZSM-12 zeolite is a one-dimensional pore zeolite with pore openings of 0.57 nm × 0.61 nm, which are between the pore size of large-pore and medium-pore zeolites, making it an interesting material for isomerization, alkylation, and the reforming of paraffins [2,3]. In the alkylation of naphthalene for the preparation of 2,6-DMN, 2,7-DMN has higher-energy diffusion barriers than 2,6-DMN in the ZSM-12 zeolite (102.6 kJ/mol and 10.9 kJ/mol, respectively) [4]. In addition, ZSM-12 showed excellent resistance to deactivation by carbonaceous deposits due to its one-dimensional pore. ZSM-12 has been predicted to be the most promising candidate for the selective alkylation of naphthalene to 2,6-DMN [5].

Acid dealumination is an important method to improve the catalytic properties of zeolites through the modification of the pore structure and surface acid properties, and leads to high hydrothermal stability [6–9]. In this work, the dealumination of HZSM-12 (Si/Al = 67) was carried out with citric acid and hydrochloric acid. A systematic investigation was carried out on the effects of citric acid and hydrochloric acid treatments on ZSM-12, including its

* Corresponding author. Tel.: +86 451 86609227; fax: +86 451 86609227.
E-mail addresses: mary.wu@tom.com, wuwei@hlju.edu.cn (W. Wu).

1381-1169/$ – see front matter © 2009 Elsevier B.V. All rights reserved.
doi:10.1016/j.molcata.2009.08.020

structure, acidic properties and catalytic behavior in the 2,6-DMN synthesis.

2. Experimental

2.1. Preparation of samples

The zeolite ZSM-12 was crystallized for 120 h using hydrothermal method at a temperature of 433 K in the autoclave with polytetrafluoroethylene inside linings, silica sol as silica source, sodium aluminate as aluminum source and tetraethylammonium bromide as template. In typical preparation, the ZSM-12 was synthesized from a reaction mixture having the composition $3.25Na_2O{:}0.77Al_2O_3{:}100SiO_2{:}12.5TEABr{:}1300H_2O$. When the autoclave is cooled and the solid is separated from the mother liquor. The as-synthesized ZSM-12 was ion-exchanged by 0.5 M NH_4NO_3 solution at room temperature for 3 h and then washed with demineralized water until the washing water has a pH of 7. This was followed by drying at 120 °C overnight. The above process was repeated three times. The NH_4-form zeolite thus obtained was calcined at 550 °C for 3 h in air to obtain HZSM-12 (these samples are labeled as PZ).

Dealumination was processed by acid leaching of 5 g of the PZ mixed with 50 mL of solution of critic acid or hydrochloric acid at reflux temperature. The samples treated by 1 mol/L, 6 mol/L, 10 mol/L hydrochloric acid for 6 h denoted HClZ1, HClZ2 and HClZ3, respectively. The samples dealuminated by 2 mol/L critic acid for 6 h, 18 h and 24 h labeled CAZ1, CAZ2 and CAZ3, respectively. The obtained zeolite samples were washed with water, dried at 120 °C for 12 h and then calcined at 520 °C for 4 h.

2.2. Characterization

X-ray powder diffraction (XRD) patterns of the modified and unmodified zeolite samples were recoded on a D/MAX-3B powder diffractometer range of 3–50° at a scanning speed of 2°/min and step size of 0.02°. The bulk composition of the samples was performed by SRS-3400 XRF (Bruker Co., Germany). Physical-absorption of nitrogen was studied using Quantachrome AUTOSORB-1-MP Automated Gas Sorption System. Prior to measurement the samples were outgassed at 300 °C for 24 h. Specific surface areas were determined using the BET equation and values of the micropore surface area, micropore volume were estimated by applying the *t*-plot method. Total pore volume was determined at about 0.99 relative pressure. To observe the crystal modification of the treated zeolite, scanning electron microscopy was carried out (D/max-IIIB). Pyridine- adsorbed Fourier transform Infrared (Py-FTIR) spectrum experiments conducted on a VECTOR22 FTIR instrument (Bruker Co., Germany) with a resolution of 4 cm^{-1}. A wafer was prepared from 30 mg of catalyst and preheated at 350 °C in vacuum, and then cooled to room temperature, followed by pyridine adsorption. Physisorbed pyridine was removed by degassing for 1 h at 150 °C in vacuum and then the FTIR were carried out at room temperature. The quantities of Brønsted acid sites and Lewis acid sites were then measured in the range of 1750–1350 cm^{-1}. NH_3 temperature-programmed desorption (NH_3-TPD) was performed on a conventional set-up equipped with a thermal conductivity detector (TCD). The catalyst charge was 0.2 g with particle size of 20–40 mesh. The sample was first treated in the flow of helium at 550 °C for 1 h, and then cooled down to 120 °C. The adsorption of NH_3 was performed with the flow of He at 120 °C. The desorption was conducted between 120 °C and 800 °C at a heating rate of 12 °C/min. ^{29}Si MAS NMR spectra were recorded on a Infinity plus 300WB (Varian Co., American).

2.3. Catalytic reaction

All experiments were carried out in a high-pressure fixed-bed down-flow microreactor with an inner diameter of 10 mm. The reactants mixture of naphthalene, 1,2,4-trimethylbenzene, methanol were injected by a high-pressure pump into the tubular stainless-steel reactor, the middle stage of which was charged with 2.0 g of catalyst in the form of granules (20–40 mesh). The catalyst was initially pretreated in situ in N_2 flow 500 °C for 1 h before reactants were injected into the reactor. The typical reaction conditions were as follows: 350 °C reaction temperature; 4.0 MPa reaction pressure; 3 h^{-1} weight hourly space velocity (WHSV, total liquid feed); 1:2:8 molar ratio of naphthalene, methanol, 1,2,4-trimehtylbenzene in liquid feed. To keep the system at steady high-pressure, 10 mL/min N_2 stream was introduced concurrently with the reaction feed into the reactor at the reactor head. Under these reaction conditions, the reaction could take place in the liquid phase. The catalytic reaction products containing mixture of 2,6-DMN were analyzed by GC on a Angilent 6890N instrument, with a SHINWA Industry WCOT PLC capillary column (50.0 m × 250 μm × 0.25 μm). The conditions of typical sample analysis were as follows: the temperature program used was a ramp beginning at 130 °C for 2 min, going to 151 °C at 2.5 °C/min and making an isotherm for 40 min. Nitrogen was used as the carrier gas. Injection and FID detector temperatures 250 °C.

The conversion and 2,6-/2,7-DMN were calculated as follows. NAPH Conv. = $(M_{NAPH0} - M_{NAPH})/M_{NAPH0} \times 100\%$, where NAPH Conv. is conversion of naphthalene, M_{NAPH0} is the molar percentage of naphthalene before reaction, and M_{ANPH} is the molar percentage of naphthalene after reaction. 2,6-/2,7-DMN stands for the molar ratio of 2,6-DMN to 2,7-DMN.

3. Results and discussion

3.1. Relative crystallinity and bulk composition

The XRD patterns of the samples are shown in Fig. 1. The bulk composition and relative crystallinity of the samples are shown in Table 1.

As shown in Fig. 1, the samples are highly crystalline after citric and hydrochloric acid leaching, as indicated by the strong intensity of the characteristic peaks that occurred at 2θ values of 7.4°, 8.8°, 20.8°, and 23.1°, which are exclusively attributed to the structure of MTW type material [10]. This suggests the different dealumination methods used did not obviously degrade the crystalline structure of the HZSM-12 zeolites.

Table 1 clearly shows that the relative crystallinity of the HZSM-12 zeolite decreases as the concentration of the hydrochloric acid increases because of the formation of amorphous phases during dealumination. It also shows the Si/Al ratios increase to 76 and

Table 1
Compositional and structural characteristics of the parent and HZSM-12 zeolites treated with acids.

Samples	Treatment method	Si/Al (atom ratio)[a]	Relative crystallinity (%)[b]
PZ	Parent	67	100
HClZ1	1 mol/L HCl, 6 h	76	90
HClZ2	6 moL/L HCl, 6 h	98	83
HClZ3	10 mol/L HCl, 6 h	90	77
CAZ1	2 mol/L CA, 6 h	67	94
CAZ2	2 mol/L CA, 18 h	78	82
CAZ3	2 mol/L CA, 24 h	88	72

[a] Calculated from X-ray fluorescence spectroscopy (XRF) data.
[b] Obtained by comparing the X-ray diffraction (XRD) peak (2θ = 18.6°, 20.64° and 22.88°) intensities of the modified samples with that of the parent ZSM-12 zeolite that considered to be 100% crystallinity.

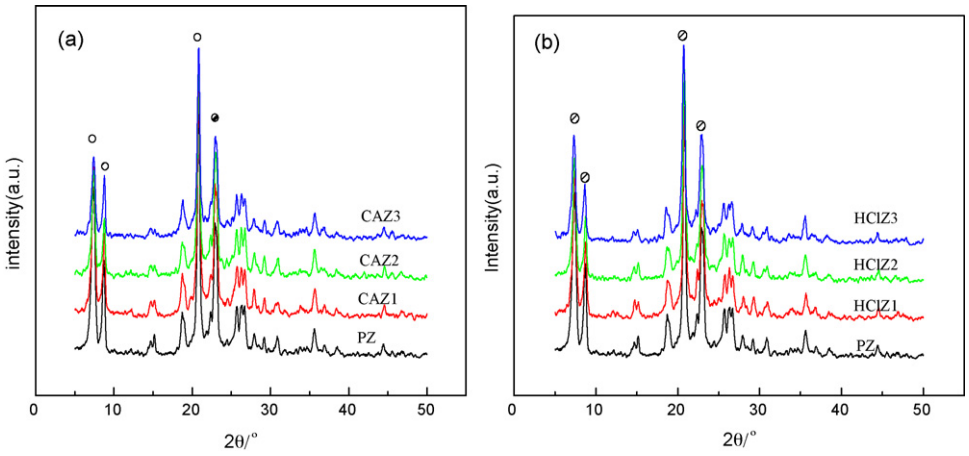

Fig. 1. XRD patterns of the parent and HZSM-12 zeolite samples treated with CA (a) and HCl (b).

98, both of which are easily reached using 1 mol/L and 6 mol/L hydrochloric acid, respectively, but ultimately the Si/Al ratio is about 90 using a 10 mol/L solution. The abnormal behavior of Si/Al ratio can be explained by the simultaneous dissolution of silica units from the framework owing to the high acidity of the solution that is at a pH of −1 in the case of 10 mol/L hydrochloric acid solution, and the degree of desilication is higher than dealumination when the highly concentrated hydrochloric acid solution is used. In previous works, Giudici et al. also showed that the hydrolysis of the silicon bonds occurred in the case of 6 mol/L nitric acid (pH −0.8) [11,12].

It is also shown that the relative crystallinity of HZSM-12 zeolite gradually decreases from 100% of the sample PZ to 94%, 82%, 72% of CAZ1, CAZ2, CAZ3, respectively, with the increase of dealumination time. For CAZ1, the relative crystallinity decreases to 94%, but no evident changes are found in the Si/Al ratios. This is because the removal of the framework aluminum results in a lattice defect in the framework of the zeolite, but the extra-framework aluminum formed did not diffuse off from the channels. With the prolonging of the dealumination time, the extra-framework aluminum diffuses off from channels gradually, leading to an increase in the Si/Al ratio.

SEM images of CAZ3 and HClZ3 in Fig. 2 show that the outer surface of the CAZ3 is essentially unchanged compared with PZ (not shown here). However, the outer surface of HClZ3 is strongly corroded and partially cracked, split in one direction, owing to the severe dealumination accompanied by desilication.

3.2. Nitrogen adsorption

For the samples PZ, HClZ3 and CAZ3, nitrogen adsorption–desorption isotherms at liquid-nitrogen temperature are presented in Fig. 3. The isotherm of the untreated ZSM-12 sample is type I with a steep uptake below $P/P_0 = 0.02$, indicating micropore filling and limited N_2 uptake at higher relative pressures. The nitrogen adsorption isotherms still contain an insignificant hysteresis loop from $P/P_0 = 0.45$ to about 0.9, which suggests secondary particle piled pores of ZSM-12 grain or local defects formed in the crystallization process. The adsorption–desorption isotherms of the sample PZ was in accord with that reported in the literature [13]. The hysteresis loops of the samples HClZ3 and CAZ3 are wider than that of PZ. When taken together, the increase of the Si/Al ratio and the reduction in the relative crystallinity after acid treatment wider hysteresis loop attributed to a compound-type of type I and IV isotherms [14], which indicates the formation of a secondary pore [15], which is probably related to the removal of the aluminum atoms in the structural defects in the framework of the zeolite.

Textural properties of untreated and acid-treated ZSM-12 samples are shown in Table 2. For HClZ1 and HClZ2, the micropore volumes slightly increase from 0.100 m^3/g of PZ to 0.102 m^3/g and to 0.101 m^3/g, when the Si/Al ratio increases from 67 to 76 and to 98, respectively. This phenomenon shows that treatment with low concentrations of hydrochloric acid can remove the aluminum oxide species that block the micropores without the destruction of the ZSM-12 framework. However, when Si/Al ratio increase to 90 for HClZ3, the micropore surface areas and the micropore volumes markedly decrease owing to the partial collapse of the structure (relative crystallinity is 77%) and to the extra-framework aluminum formed. In contrast to these results, the micropore volumes and micropore areas of all samples of the citric acid-treated HZSM-12 are larger than PZ because the coordination compound of citric acid and alumina, including framework alumina and extra-framework alumina, could escape from the channels [16], thus the channels are

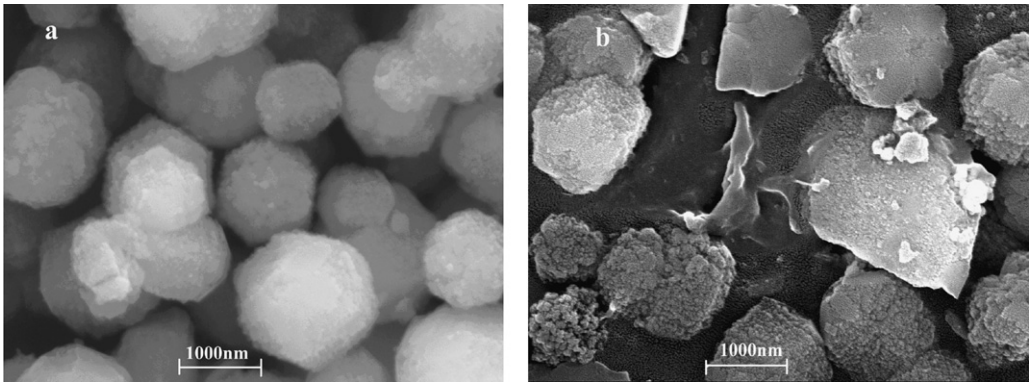

Fig. 2. SEM micrographs of the dealuminated HZSM-12 zeolite samples CAZ3 (a) and HClZ3 (b).

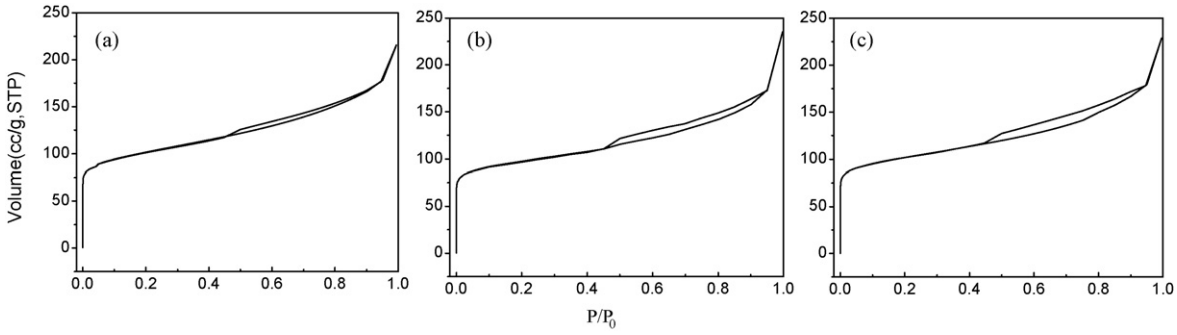

Fig. 3. Nitrogen adsorption-desorption isotherms of the parent (a) and dealuminated HZSM-12 zeolite samples HClZ3 (b) and CAZ3 (c).

dredged, which is beneficial to the reactants and products diffusion and improves the catalytic performance. The degree of dealumination is further strengthened by the time of the treatment, and the secondary pore structure is formed without the destruction of the framework structure.

3.3. NH_3 temperature-programmed desorption and FTIR of pyridine adsorption

Fig. 4 shows the NH_3-TPD results of the dealuminated samples. Three peaks of ammonia desorption are observed on the curves. Among them, the peaks at 170 °C, 300 °C, and 380 °C are assigned to the ammonia desorbed from the weak, medium and strong acid sites, respectively. Sample HClZ1 has a larger number of acid sites than PZ because the low concentration of hydrochloric acid removed the aluminum oxide species, which block the micropores, therefore, more acid sites are exposed. For sample HClZ3, the number of acid sites, including weak, medium and strong acid sites, significantly decreased when compared with PZ, but the acid strength made no significant difference. This phenomenon indicates that the high concentration of hydrochloric acid eliminates the same number of weak and strong acid sites, simultaneously. In contrast, for sample CAZ1, the medium and strong acid sites significantly decrease without any change in the number of weak acid sites denoting citric acid preferentially eliminates the strong acid sites. By prolonging the dealumination time to 24 h, the weak acid sites also begin to decrease.

For the two series of HZSM-12 treated by citric acid and hydrochloric acid, the acidity of the Brønsted and Lewis sites after the adsorption of pyridine at 150 °C are shown by the intensity of the infrared absorption band in Fig. 5 and Table 3.

As shown in Table 3, the number of acid sites in sample CAZ3 is larger than that of HClZ3, but interestingly the Si/Al ratio of the two samples is similar. This finding is different from the results of the other papers and the traditional concept that a high number of acid sites corresponds to high Al concentration (low Si/Al ratio). This can be explained by the fact that the framework aluminum is removed from the crystal lattice of ZSM-12 zeolite by hydrochloric acid to form extra-framework non-acid aluminum species, which could not be wiped from the channels, therefore, the Si/Al ratio is similar to CAZ3, but the number of acid sites has decreased. As shown in Fig. 5, the peaks at 1541 cm^{-1} and 1447 cm^{-1} can be attributed to the Brønsted acid sites and Lewis acid sites, respectively, while the signal at 1491 cm^{-1} is attributed to the overlap of these two types of acid sites. According to Fig. 5, post-treatment all the samples show a decrease in their absorbance at 1541 cm^{-1}, indicating that each route of dealumination has an effect on the elimination of Brønsted acid sites in the ZSM-12 zeolite. Because the Brønsted acid sites come from $O_3Si–OH–AlO_3$ structure [17,18] provided by the framework aluminum, thus dealumination mainly occurred in the framework aluminum. On the other hand, the amount of Lewis acid sites of HClZ3 is similar to PZ because the forms of the extra-framework aluminum are neutral or polymeric aluminum species, e.g., $AlO(OH)$, $Al(OH)_3$, and Al_2O_3. Additionally, the number of Lewis acid sites in CAZ3 is larger than PZ due to the forms of the extra-framework aluminum is Lewis acidity, e.g., Al^{3+}, AlO^+, $Al(OH)_2$, and $Al(OH)_2^+$ [16], thus the value of L acid/B acid increased significantly.

3.4. ^{29}Si MAS NMR

The ^{29}Si MAS NMR spectra of the PZ and CAZ3 samples are shown in Fig. 6. In both of the samples, the two lines centered at around −113 ppm and −105 ppm are ascribed to the Si(0 A l) and Si(1 A l) crystallographic sites, respectively. Changes in the intensities of the peaks are observed after citric acid dealumination. The intensity of the Si(1 A l) signal decreased, but the intensity of the Si(0 A l) signal increased. It is shown that the framework Si/Al ratio was increased resulting in dealuminating framework aluminium.

Because the Brønsted acid sites are mainly provided by the $O_3Si–OH–AlO_3$ structure (i.e., Si(1 A l) sites), acid dealumination can reduce the number of Brønsted acid sites. Moreover, we do not observe the peak at around −100 ppm, which is ascribed to the

Table 2
Textural properties of the parent and HZSM-12 zeolites treated with HCl and CA.

Sample	Surface area (m^2/g)			Pore volume (cm^3/g)		
	BET[a]	External	Micropore[b]	Total[c]	Mesopore	Micropore [b]
PZ	371	137	234	0.335	0.235	0.100
HClZ1	357	107	250	0.298	0.196	0.102
HClZ2	353	103	250	0.309	0.208	0.101
HClZ3	365	137	228	0.269	0.180	0.089
CAZ1	396	141	255	0.387	0.286	0.101
CAZ2	365	114	251	0.321	0.218	0.103
CAZ3	379	122	257	0.355	0.249	0.107

[a] BET method.
[b] *t*-Plot method.
[c] Volume adsorbed at $P/P_0 = 0.99$.

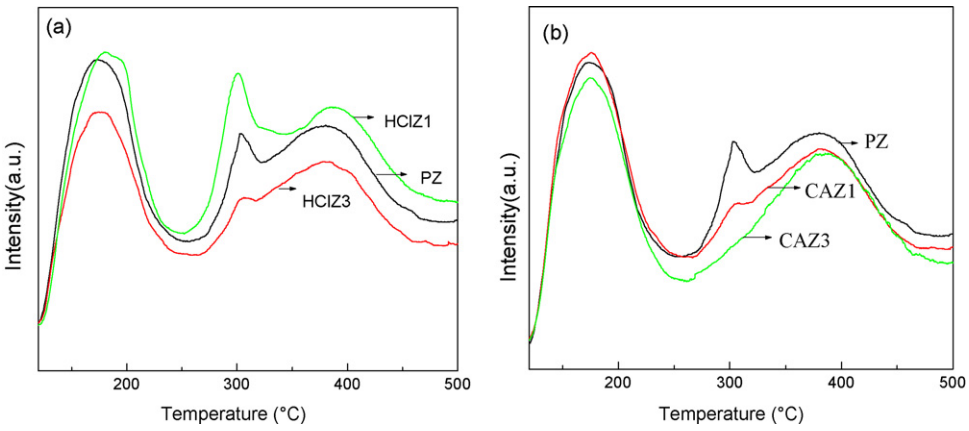

Fig. 4. NH_3-TPD profiles for parent and HZSM-12 zeolite samples treated with HCl (a) and CA (b).

Table 3
The acid distribution of the parent and dealuminated HZSM-12 zeolites CAZ3 and HClZ3.

Samples	Si/Al	Total acidity (mmol g^{-1})	Brønsted acidity (mmol g^{-1})	Lewis acidity (mmol g^{-1})	L/B acidity
PZ	65	0.55	0.24	0.31	1.30
CAZ3	88	0.48	0.10	0.38	3.89
HClZ3	90	0.43	0.13	0.30	2.22

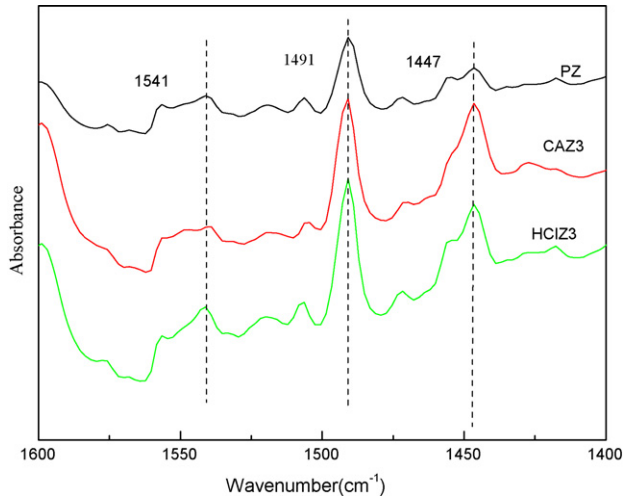

Fig. 5. Pyridine adsorbed FTIR spectra of the parent and dealuminated HZSM-12 zeolite samples CAZ3 and HClZ3.

Si(2 A l) signal in both samples. Because the samples in this work are a high silica zeolite, the Si(0 A l) is the chief chemical environment of the silicon atoms.

3.5. *Methylation of naphthalene over dealuminated zeolites*

The methylation of naphthalene with methanol over the HClZ3 and CAZ3 catalysts was carried out. Figs. 7 and 8 and Table 4 show the conversion of NAPH, product distribution and 2,6/2,7-DMN ratio with time on stream (TOS).

As shown in Figs. 7 and 8, the catalytic stability of the PZ is lower, and the conversion of naphthalene decreases quickly under the high initial activity. The initial activity of the dealuminated samples are lowered because of the less active centers, whereas the catalytic stability was improved markedly, the conversion of naphthalene over samples HClZ1, HClZ2 and CAZ2 is significantly higher than with PZ after 4 h of the reaction. This may be attributed to a decrease in the strong acid sites of the dealuminated samples which conduced to restrain coke formation (as shown in Fig. 9). On the other hand, the diffusion of products was improved by application of the dealumination as a promising alternative to increase (meso)porosity in ZSM-12 zeolites. Secondary mesopores reduces

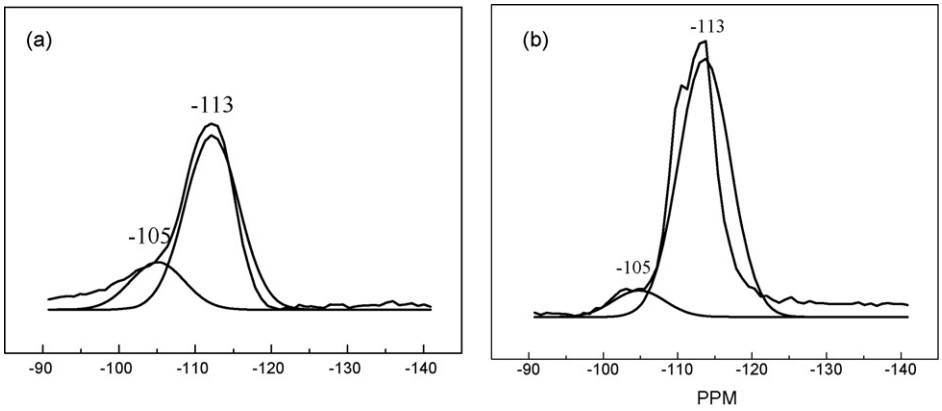

Fig. 6. ^{29}Si MAS NMR spectra of the parent (a) and dealuminated HZSM-12 zeolite sample CAZ3 (b).

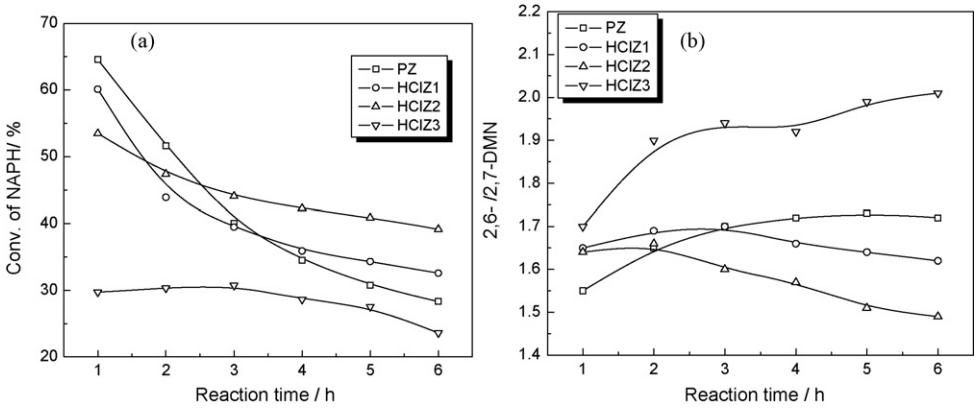

Fig. 7. Effect of dealuminated HZSM-12 zeolite samples by HCl on the conversion of NAPH (a) and 2,6-/2,7-DMN ratio (b).

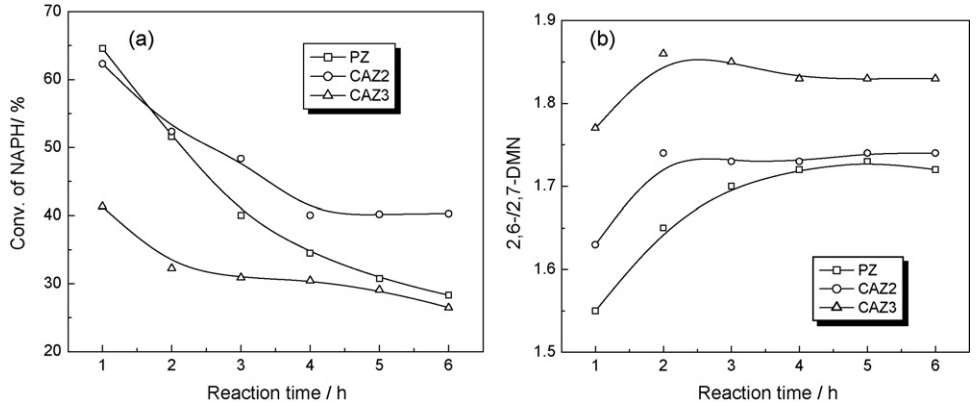

Fig. 8. Effect of dealuminated HZSM-12 zeolite samples by CA on the conversion of NAPH (a) and 2,6-/2,7-DMN ratio (b).

the diffusion resistance and correspondingly increases the diffusion rate of the feed and reaction products, thus finally leading to the significant improvement of the conversion of naphthalene. Figs. 7 and 8 and Table 4 show lower activity and higher catalytic stability of the HClZ3 and CAZ3 samples, highest 2,6-DMN molar percentages of 28.9% and 2,6-/2,7-DMN ratio of 1.92 were obtained at 4 h over the HClZ3 sample. First, this may be attributed to intensify the effect of electron density distinction between positions 6 and 7 in 2-MN molecule (negative ESP charge was −0.088 and −0.049, respectively [19]) over the catalyst HClZ3 having less strong acid sites, carbocation produced from methanol possesses higher activity to attack positions 6 in intermediate product of methylation of naphthalene with methanol, 2-MN molecule than the positions 7. Therefore, weaker acid sites prefer to produce 2,6-DMN than 2,7-DMN. Second, dealumination generated secondary mesopores modified diffusion of 2,6-DMN having larger dimension than 2,7-DMN (6.44 × 2.76 × 10.1 Å and 6.03 × 2.76 × 9.7 Å, respectively) [20], which leading to increase the 2,6-DMN/2,7-DMN ratio.

Fig. 9 shows the weight loss curves of the used catalysts samples PZ and dealuminated by HCl and CA. It is seen that with the increases of concentration of HCl or treated time by CA, the amount of coke formed on the catalysts decreases, the lost amount of coke

Table 4
Catalytic performance of PZ and dealuminated catalysts in the alkylation of NAPH with methanol.

	PZ	CAZ2	CAZ3	HClZ1	HClZ2	HClZ3	Therm[a]
NAPH conversion (%)	34.5	40.0	30.5	35.9	42.3	28.6	–
Product distribution (mol%)							
MN	63.0	54.1	74.1	73.7	66.5	76.1	–
DMN	28.3	35.6	22.3	23.3	26.9	20.6	–
TMN^{+}	8.7	10.3	3.6	3.0	6.6	3.3	–
DMN distribution (mol%)							
2,6-DMN	25.7	24.5	25.0	23.7	23.0	28.9	12.0
2,7-DMN	15.0	14.2	13.7	14.3	14.5	15.0	11.7
2,3-DMN	3.9	4.8	4.7	4.1	4.4	4.0	12.1
1,2-DMN	5.4	9.3	7.5	9.8	13.2	4.2	9.7
1,3-DMN	8.5	8.0	9.1	9.2	8.7	8.9	14.8
1,6-DMN	23.9	21.8	23.0	23.3	21.4	25.8	14.0
1,7-DMN	12.8	12.2	11.9	12.1	11.6	13.2	14.7
1,4- and 1,5-DMN	4.8	5.2	5.1	3.5	3.2	0	11.0
2,6-/2,7-DMN	1.72	1.73	1.83	1.67	1.57	1.92	1.0

T = 350 °C; P = 4 MPa; N_2 = 10 mL/min; NAPH:CH_3OH:1,2,4-TMB = 1:2:8 (mol); WHSV = 3 h^{-1}; time = 4 h.

[a] Thermodynamic equilibrium value.

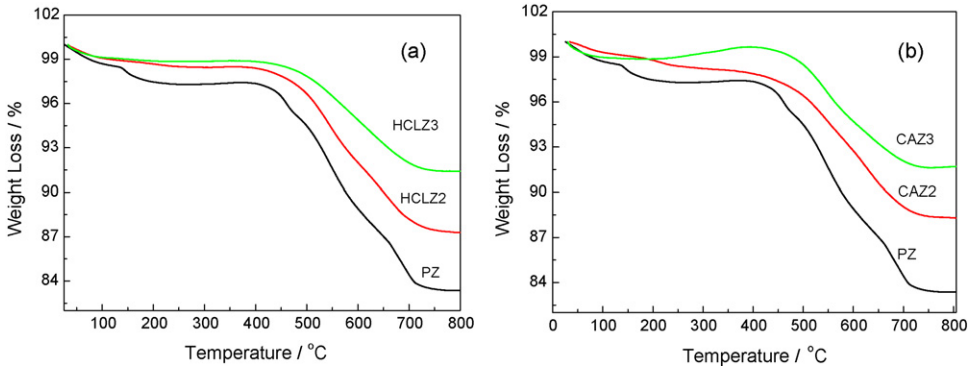

Fig. 9. The curves of the parent and HZSM-12 zeolite samples treated with HCl (a) and CA (b).

is about 8.5% for the used catalyst HClZ3 was obtained which bring highest catalytic stability.

4. Conclusions

(1) Dealumination of HZSM-12 with hydrochloric acid and citric acid has different effects on the pore structure, acidic properties and catalyst preference. Hydrochloric acid eliminates the strong and weak acid sites simultaneously, without destroying the skeleton structure of the zeolite and improving the catalytic activity and stability. Treatment of HZSM-12 zeolite by 10 mol/L HCl induces severe dealumination associated with desilication, the amount of acid sites of the sample HClZ3 was markedly reduced, resulting in a lower conversion of naphthalene, but the catalytic stability, 2,6-DMN molar percentages and 2,6-/2,7-DMN ratio were significantly improved.

(2) Treatment of HZSM-12 zeolite by 2 mol/L citric acid preferred to eliminate the strong Brønsted acid sites on the framework aluminum, as well as, to increase the microporous volume and form secondary pores. The results show that the sample CAZ2 dealuminated HZSM-12 zeolite by 2 mol/L citric acid for 18 h obtained higher catalytic activity for the methylation of naphthalene with methanol.

Acknowledgements

This work is supported by the National Nature Science Foundation of China (No. 20376012) and Heilongjiang Science and Technology Plan (No. WC05A10).

Appendix A. Supplementary data

Supplementary data associated with this article can be found, in the online version, at doi:10.1016/j.molcata.2009.08.020.

References

[1] Z.R. He, L.H. Zhu, Coal Chem. Ind. 94 (2001) 51–56.
[2] W.M. Zhang, P.G. Smirniotis, Catal. Lett. 60 (1999) 223–228.
[3] S. Gopal, W.M. Zhang, P.G. Smirniotis, Ind. Eng. Chem. Res. 43 (2004) 2950–2956.
[4] R. Millin, F. Frigerio, G. Bellussi, J. Catal. 217 (2003) 298–309.
[5] G. Pazzucconi, C. Perego, R. Millini, F. Frigerio. US 6,147,270, 2000-11-14.
[6] C.S. Triantafillidis, N.P. Evmiridis, Ind. Eng. Chem. Res. 39 (2000) 3233–3240.
[7] J. Datka, S. Marschmeyer, T. Neubauer, J. Meusinger, J. Phys. Chem. 100 (1996) 14451–14456.
[8] N. Viswanadham, J.K. Gupta, G. Murali Dhar, Energy Fuels 20 (2006) 1806–1814.
[9] N. Viswanadham, L. Dixita, J.K. Guptaa, M.O. Garg, J. Mol. Catal. A: Chem. 258 (2006) 15–21.
[10] C.A. Fyfe, H. Gies, G.T. Kokotailo, J. Phys. Chem. 94 (1990) 3718–3721.
[11] R. Giudici, H.W. Kouwenhoven, R. Prins, Appl. Catal. A: Gen. 203 (2000) 101–110.
[12] F. Wolf, H. John, Chem. Technol. 25 (1973) 736–741.
[13] X.T. Tong, G.P. Smirniotis, Micropor. Mesopor. Mater. 89 (2006) 170–178.
[14] R.Q. Lu, J. Gu, B. Tan, et al., J. Fuel Chem. Technol. 32 (2004) 504–509.
[15] H.A. jot, J.F. Joly, J. Lynch, et al., Stud. Surf. Sci. Catal. 62 (1991) 583–587.
[16] Z.K. Xie, Q.L. Chen, C.F. Zhang, J. Phys. Chem. B 104 (2000) 2853–2859.
[17] W.O. Haag, R.M. Lago, P.B. Weisz, Nature 309 (1984) 589–591.
[18] D.P.B. Peixotoa, S.M. Cabral de Menezesb, M.I. Pais da Silva, Mater. Lett. 57 (2003) 3933–3942.
[19] C. Zhang, X.W. Guo, C.S. Song, Chin. Chem. Lett. 18 (2007) 1281–1284.
[20] Y. Fang, H. Hu, Catal. Commun. 7 (2006) 264–267.